Med Biol Eng Comput (2009) 47:515–522
DOI 10.1007/s11517-009-0483-7

SPECIAL ISSUE - ORIGINAL ARTICLE

Refixation stability in shoulder hemiarthroplasty in case of four-part proximal humeral fracture

Daniel Baumgartner · Silvio René Lorenzetti · Robert Mathys · Beat Gasser · Edgar Stüssi

Received: 9 July 2008 / Accepted: 27 March 2009 / Published online: 1 May 2009

Abstract Primary stability of refixated fractures in case of shoulder hemiarthroplasty is a prerequisite to restore physiological glenohumeral joint function. Clinical observations often show a secondary dislocation and subsequent resorption of the bony anchor points like the greater and lesser tuberosity at the rotator cuff tendons. This failed integration leads to impaired glenohumeral load transmission and subsequent reduction of mobility. As a consequence, the optimisation of refixation methods is crucial for a better clinical outcome. To prove the stability of refixation techniques, a Finite Element fracture model was built. Resulting stresses at the bone surface and fragment migration relative to the prosthesis shaft were studied. The results of the calculations show that the isolated tuberosities show unstressed bone regions compared to the intact model. This circumstance may explain the clinically detected bone resorption due to the absence of mechanical stimuli. Furthermore, a cable guidance through lateral holes in the middle part of the proximal prosthesis results in a lower fragment displacement than a circumferential fixation method surrounding the entire proximal bone.

Keywords Shoulder prosthesis · Hemiarthroplasty · Proximal humeral fracture · Tuberosity fixation · Cerclage technique

D. Baumgartner (✉) · S. R. Lorenzetti · E. Stüssi
ETH Zürich, Institute for Biomechanics, HCI E 451,
Wolfgang Pauli Strasse 10, 8093 Zurich, Switzerland
e-mail: dbaumgartner@ethz.ch

R. Mathys · B. Gasser
RMS Foundation, Bischmattstrasse 12,
2544 Bettlach, Switzerland

1 Introduction

Hemiarthroplasty represents an established treatment method for three- and four-part fractures at the proximal humerus. A great variation in clinical outcome is reported in literature. Contradictory results range from bad/satisfactory to good/excellent with regard to the Constant Score; resorption or secondary dislocation of the refixated tuberosities is shown in 30–70% of all cases [8, 18, 21–23, 28, 38, 40, 41, 44]. The refixated fragments at the proximal humeral head are often affected by non-unions and osteonecrosis [31]. The loss of muscular anchor points of the supraspinatus (SSP), infraspinatus (ISP) and subscapularis (SSC) muscles negatively affects glenohumeral load transfer and therefore postoperative shoulder function. Boileau et al. and Kralinger et al. showed in their studies that a satisfactory bone ingrowth of the greater and lesser tuberosity significantly increases clinical outcome when considering the constant score [6, 27]. This circumstance is supported by the fact that a displacement with subsequent malunion of the greater tuberosity correlates with an insufficient clinical result [34]. It has also been attempted to correlate different parameters such as prosthesis position or fragment placement with unsatisfactory clinical outcomes. As a consequence, a non-anatomical reconstruction is predisposed to even worse clinical results [2, 9, 13, 19, 26]. Unpredictable outcome of hemiarthroplasty is as well explained by the infrequency of such fractures combined with the lack of experience by the surgeon [6]. No correlation between prosthesis design and outcome was detected [29], but healing of the tuberosities appears to be crucial for achieving good function in patients treated with a humeral head prosthesis [37]. As a technical parameter, the refixation technique seems to be essential for a tuberosity union [6, 15, 25] and primary interfragmentary stability is

considered to be one of the most influencing factors affecting the outcome [33].

Until now, the initial failure mechanism of a cerclage construct is not clear. On the one hand, a displacement of the tuberosity fragments may be the reason for subsequent bone resorption, on the other, a primary loss of bone stock and volume reduction at the proximal humerus reduces the cerclage tension and may lead to fragment migration. Conditions leading to optimised bone ingrowth are primarily proven based on standardised experimental or mathematical models. To our knowledge, there is no literature available that correlates stable fragment placement with an optimised bone ingrowth at the fractured proximal humerus.

Two factors have to be fulfilled for a successful bone ingrowth considering an implant-to-bone interface [3]. An appropriate biocompatibility of the implant material on the one hand [4] and the initial stability of the bone fragment on the implant on the other. A stable immediate (primary) fixation is a requirement for a successful osseous integration and subsequent secondary stability [36].

Beside the adaptation of the bone to the prosthesis surface, the relative interfragmentary movement is of importance for a successful healing process. An oversized fracture gap distance may negatively influence the vascular system reorganisation. The proximal humerus is vascularised by an intensive intraosseous arterial distribution [17]. Some vessel branches on the humeral surface are oriented orthogonally to the surgical neck fracture line; parallel to the longitudinal axis of the bone [10, 17, 24, 32]. A fracture tends to interrupt the interconnective system and may lead to avascular necrosis particularly in the head fragment. Whether the fracture gap in the surgical neck or the gap in the bicipital groove negatively influences supply is not shown.

Experimental in vitro testing of tuberosity fragment stability was performed either in load-to-failure tests [1, 12] or in cyclic loading considering the fragment migration [7, 16]. A recently published study used the same prosthesis design and similar muscular loading of SSP, ISP and SSC. Interfragmentary displacements of 0.04–0.14 mm were measured [14].

Existing Finite Element Analysis (FEA) considered the reconstruction of the proximal humerus by osteosynthesis plates and screws in comparison to a nailing system [30, 39]. Some studies investigated the glenohumeral load transfer and the appearance of contact stresses in the articulating surface during abduction for the healthy joint [11, 20]. The aim of present study is an optimisation of different refixation techniques by means of a reproducible Finite Element Model with respect to an enhanced interfragmentary stabilisation. To our knowledge, no study exists up to now for investigating different refixation techniques at the proximal humerus using FE simulation methods. This paper presents a novel investigation to evaluate the quality of a refixation technique in the case of shoulder hemiarthroplasty after proximal humeral head fracture.

2 Materials and methods

The present FE study is based on a four-part fracture model of the proximal humerus. The fragments are defined by the greater and lesser tuberosity, the humeral stem and the articulating surface of the humeral head, whereas last-mentioned fragment is replaced by the artificial surface of the implant. A commercially available artificial prosthesis was inserted simulating a hemiarthroplasty. Three refixation techniques were studied and evaluated with respect to the fragment stability and resultant stresses on the bone. The following assumptions were made for the calculations:

2.1 Implant and bone geometry

Implant geometry was built based on the Affinis Fracture Prosthesis (Mathys Ltd. Bettlach, Switzerland) [37]. The overall shape of the prosthesis, middle shaft, the stem and the head, was considered as one uniform rigid body model. The coating revealing a microstructure for a better bone ingrowth was not taken into account. Humeral proximal bone shape was reconstructed based on CT scans with a simplification of the geometry using spherical and conic surfaces (concave parts like the bicipital groove were not implemented). The approximate diameter of the humeral head (in a horizontal plane cross-section through the humeral head centre) was 38 mm.

A global coordinate system was set to define the orientation in the space: the z-axis of the coordinate system was collinear to the centreline of the cylindrical prosthesis shaft in cranial direction. The x-axis was medially directed, within in the frontal plane. As a result, the y-axis pointed dorsally.

An idealised four-part fracture model was simulated and built in CAD Unigraphics NX 4.0 according to existing literature [16]. The humeral head fragment including the articulating surface is replaced by the prosthesis surface, whereas greater and lesser tuberosity fragment are reattached laterally at the prosthesis middle part. The defined fracture borderlines splitting up the proximal humerus into the single fragments were built by planes: The plane which defined the fracture through the bicipital groove included the central vertical axis of the prosthesis shaft and was rotated 30° around the positive z-axis. The plane defining the surgical neck fracture of the humeral head was tilted around the positive y-axis of 15° (Fig. 1). As a

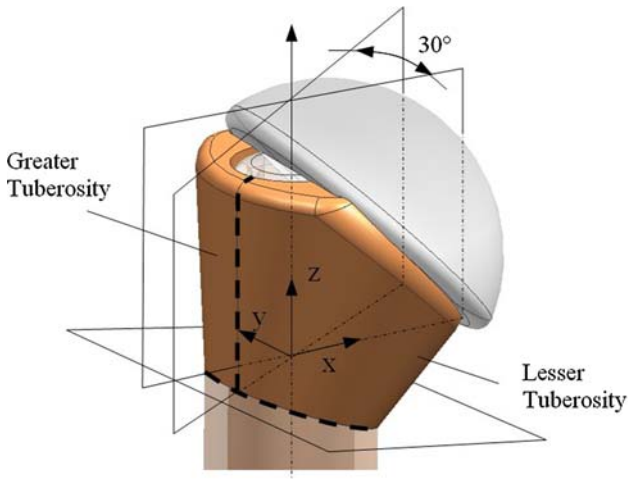

Fig. 1 Geometry of a four-part fracture model on a left humerus according to [16]

consequence, the fragments were not interlocked by a rough and uneven interface.

2.2 Refixation techniques

Three different refixation methods were tested: Type A consists of two cerclages around the greater and lesser tuberosity fragment parts, surrounding the whole fractured proximal humerus; Type B comprises two cerclages guided through anteroposterior prosthesis holes located in the middle part; Type C includes a crossover of the cable on the lateral bone surface of the proximal humerus (Fig. 2). These three fractured models were compared with an ideal situation used as a control without a fracture gap and with no cables around the bone but with the prosthesis implanted. This circumstance represents an already healed situation, which refers to a desired postoperative result. It has been taken into account that the total cable length of each of the refixation types did not vary in a great extent; total cable length including both cerclages was 220 mm for Type A, 163 mm for Type B and 173 mm for Type C.

To simulate the cable guidance on the bone surface, predefined grooves were assumed not allowing lateral shifting. The grooves had a depth of 0.5 mm, which represented half of the cable diameter (Fig. 3). The concavity of the groove corresponds to the convex shape of the cable; a perfect form fit was therefore defined between the cable and the groove interface.

2.3 Material properties

The implant's middle part made of titanium and the ceramic head were considered as one rigid body. Cortical and cancellous bone material properties were taken from literature [35]; the elastic modulus of cortical bone $E = 6.0$ GPa, cancellous bone $E = 0.7$ GPa, the Poisson's ratio was homogenously defined as $\nu = 0.3$. The presence of a subchondral bone layer or articular cartilage was not implemented in this model as well as the interconnecting ligament structure at the glenohumeral joint. Steel cables were modelled according to the existing biomechanical experiments [12]. Although the used flexible cables consist of several filaments, a fully homogenous cross-section was assumed. No wire pretension was applied, simulating an already relaxed situation of the construction. We consider that assumption as a reliable condition, unless a tissue adaptation occurs after tightening the cable. A continuous cylindrical shape was used for the stem comprising a constant cross-section.

2.4 Loading conditions

The model refers to a static arm position for a 30° glenohumeral abduction angle. The rotator cuff muscle m. SSP contributes to an abduction movement, whereas m. SSC and m. ISP are controlling an in-plane scapular movement, and therefore act as lateral stabilisers. The absolute values of 24 N for the SSC, 12 N for the SSP and 6 N for the ISP were applied to the fragments. Mentioned forces refer to calculated tensile forces at the rotator cuff [42].

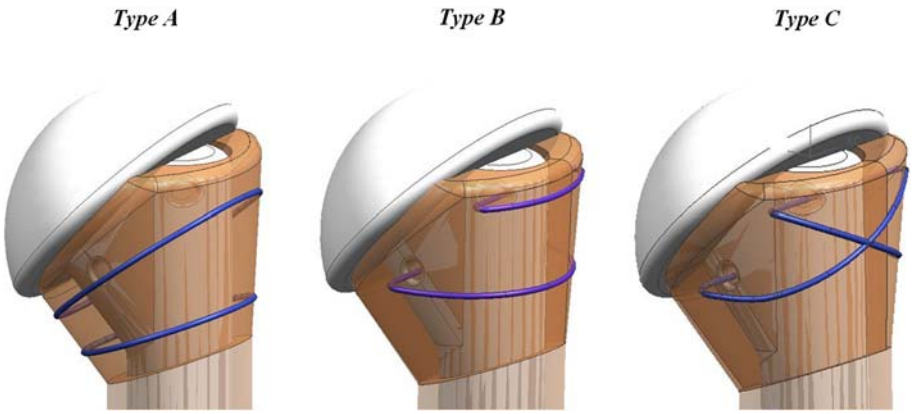

Fig. 2 Refixation methods around the fractured humerus. Type A: circumferential cerclage around the whole fractured proximal humerus, Type B: cable guidance through the prosthesis middle part, Type C: crossing of the cable on the lateral bone surface

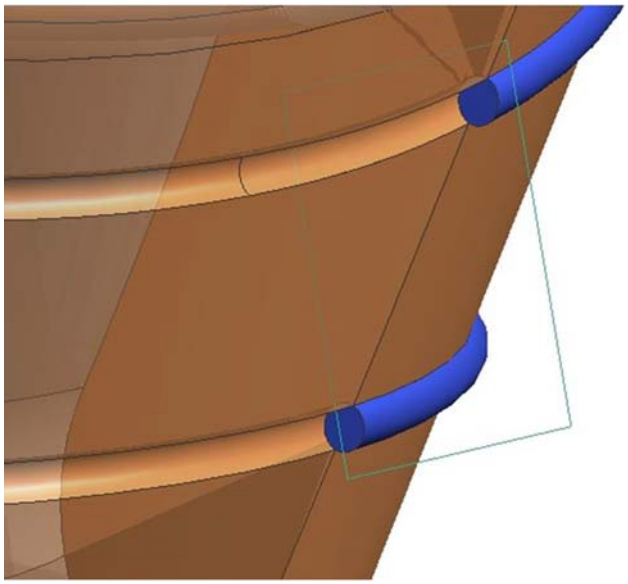

Fig. 3 A cross-section orthogonal to the cable direction is shown. The cable guidance is performed by a groove with a depth of half the cable diameter and prevents lateral shifting

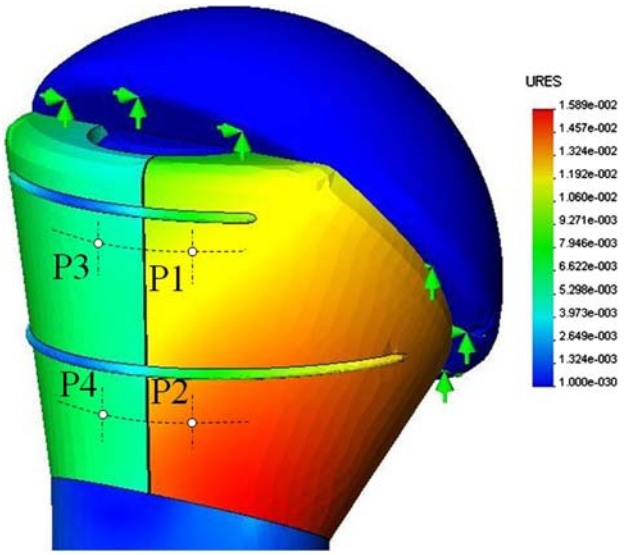

Fig. 4 Illustration of proximal humeral fragment displacement. P1 and P2 were taken as reference (undisplaced regions are coloured *blue*, maximum displacement is shown in *red*)

All muscular forces had the same direction and pointed in positive *x*-axis; therefore, the lines of action are parallel to each other. This assumption was made according to existing models [12]. These data correspond to a free hanging arm model without any support by an arm brace like in postoperative rehabilitation. Individual muscular forces were evenly distributed over the lateral surface of the greater and lesser tuberosities and introduced on all surface nodes. The prosthesis shaft comprising the head as an entire rigid body was fixed; displacements were defined equal to zero. Therefore, no counteracting glenohumeral joint force introduced at the prosthesis head was necessary to hold the system in equilibrium.

2.5 Finite element calculations

Calculations for the continuum finite element model were done by the MSC Nastran Solver. Cosmos Design Star V 4.5 was used as the pre- and postprocessor. Frictionless implant-to-fragment and cable-to-bone interaction was modelled. This condition refers to an initial postoperative situation, where an osseous bonding on the prosthesis surface is not yet generated. As a consequence, the only parameters preventing a tuberosity dislocation were the cerclage around the fragments, and the geometric form fit at the prosthesis-to-fragment interface. Due to the fact that the greater tuberosity embraces the prosthesis to a greater extent, less displacement is expected in comparison to the lesser tuberosity.

A tetrahedral mesh was used resulting in a total of approximately 50,000 linear elements which refers to an amount of 80,000 nodes. The influence of a mesh refinement (increase of the amount of elements about 20%) on the resulting stresses was calculated for one single case (Type A) but showed a negligible effect.

As output parameters, von Mises stresses were calculated as well as the resultant displacements of the specified points P1 and P2 on the lesser tuberosity and P3 and P4 at the greater tuberosity surface. P1 and P2 were located 5 mm and 25 mm below the upper horizontal fracture line, both in a distance of 10 mm anteriorly from the frontal plane. P3 and P4 had the same vertical distance to the horizontal upper fracture line, and were located in the intersection line between the frontal plane and the greater tuberosity fragment (Fig. 4). Additional points located on the inner bone surface in direct contact to the implant were analysed: P1′–P4′ represent the projected points P1–P4 on the inner bone surface, intersecting a perpendicular line to the bone surface through the given points P1–P4.

3 Results

Generally, refixated fragments are characterised by the absence of stresses compared to the healed bone in the control specimen. The differences in the amount of acting stresses between the three refixation models were not distinctive and varied in a range of 10–20%. Von Mises stresses were similar for all calculated locations P1–P4 (Table 2).

In the intact, healed model, displacements are up to an order of magnitude smaller than in the fractured models. Generally, the displacement of the greater tuberosity is

Table 1 Experimental testing of fragment displacement using the same prosthesis design compared to our investigation

Dietz [14]	Fragment distances	Sutures and cable	Only sutures
Interfragmentary displacement (μm)	LT-GT	40 (20–100)	140 (80–280)

Table 2 Von Mises stresses σ (Pa) and displacements d (μm) at locations P1 and P2 at the lesser tuberosity

Location: lesser tuberosity		Healed bone (control)	Type A	Type B	Type C
Stresses	P1	18,000	211	200	180
	P2	6,100	271	250	217
Displacements	P1	2.0	79	15	22
	P1′	1.8	46	7.9	18.4
	P2	1.8	52	10	18
	P2′	1.6	59	8.2	16.7

Table 3 Von Mises stresses σ (Pa) and displacements d (μm) at locations P3 and P4 on the greater tuberosity

Location: greater tuberosity		Healed bone (control)	Type A	Type B	Type C
Stresses	P3	27,000	243	202	178
	P4	16,000	243	215	176
Displacements	P3	3.2	4.3	5.2	7.2
	P3′	3.1	4.15	4.9	7.0
	P4	3.1	4.3	4.8	6.8
	P4′	2.9	4.2	3.9	4.5

reduced compared to the lesser tuberosity. Therefore, the lesser tuberosity seems to be more sensitive for a comparison of different refixation types with respect to the stability. Lesser tuberosity fragment displacement was up to five times higher in refixation type A compared to type B with respect to the locations P1 and P2. This effect was also seen when comparing type A to type C, where type C showed three times smaller displacements (Table 1). This circumstance was not detected for the greater tuberosity; similar displacements for all three types of refixation were seen. Displacements for the points P1′–P4′ were detected in a similar range like the exterior points P1–P4 (Tables 2, 3). As a consequence, interfragmentary deformations of the fragments can be neglected in that model for the applied load.

The rear of the rigid humeral head of the prosthesis prevented a further displacement of the fragments in the proximal region. As a consequence, a slight fragment rotation occurred primarily around the positive y-axis for the greater tuberosity and around the negative y-axis for the lesser tuberosity.

4 Discussion

The purpose of this study is to compare different refixation methods of the fractured proximal humerus with regard to resulting interfragmentary displacements as well as the stresses on the bone surface. The interrupted load transmission in the osseous structure due to the presence of a fracture gap leads to unloaded regions of the bone fragment in comparison to the healed situation (control) without fracture gaps. Despite a small displacement of the fragments, unloaded regions are characteristic for all types of cerclages. It seems that the fragment borderlines prevent any transmission of the induced stresses by muscular tension at the rotator cuff. Unfortunately, no investigation exists which describes the geometric localisation of initial in vivo bone loss at the tuberosities. This information would help to correlate clinically detected bone loss with the stress distribution in the FE model, and therefore define favourable conditions for bone ingrowth. Whether a more stable refixation leads to a better bone ingrowth at the proximal humerus is still unknown; conditions for an optimised in vivo bone formation are dependent on various parameters. But this loss of mechanical stimuli may explain the clinically observed bone resorption [43]. We have seen in our study that a smaller interfragmentary displacement due to a stable reconstruction tends to have more stresses at the defined locations on the bone surface. This circumstance was primarily seen for the greater tuberosity and could indicate that a stable fixation is needed for the transmission of higher stresses.

Generally, the greater tuberosity shows less displacement in comparison to the lesser tuberosity due to its embracing geometry surrounding the prosthesis middle part. Refixation types B and C contribute to a higher stability concerning the lesser tuberosity displacement. It remains unknown whether this circumstance is crucial for a better bone ingrowth. The results seem to follow reasonable considerations if we compare the different refixation types; in refixation type A, fewer constraints are acting because the cerclage only embraces the fragments without a direct bonding to the prosthesis. The interlocking and more constrained fixation through the prosthesis shaft in form of a tension band like in types B and C seems to provide a stabilising effect. Type C shows slightly higher displacements than type B, which could be reasonably explained by an increased overall cable length and tendency to a higher deformation. Despite the fact that some investigated refixation types show less migration, clinical decision criteria like intraoperative access and damage to the soft tissue, which surrounds the proximal humerus may be more important factors to be taken into account than the application of a technically optimised refixation type.

The applied muscular loads are in a small range. We tried to implement as well a higher loading regime in the present simulation; unfortunately, the deformation was in a high range and the iteration process during FE calculation did not succeed. Higher loads would be of interest as well to detect initial failure mechanisms of the cerclage-to-bone construct.

Some limitations in the FE model have to be accepted. It can be assumed that this simulated frictionless bone-to-prosthesis interaction reduces the overall fragment stability and accentuates the contribution of the cerclage to an enhanced stabilising effect. In further investigations, the presence of a microstructure on the prosthesis surface has to be discussed to meet the technical conditions. Due to the fact that the load direction acts parallel to the fragment-to-prosthesis interface, interlocking shearing forces may prevent a further displacement. As a consequence, we consider our model as a technical stability test and not as a model, which meets all boundary conditions according to the physiology. It is therefore to note that our worst case model reveals the highest displacements because of the absence of friction.

As a mayor limitation, the specific shaft design has to be mentioned. Our findings of the fragment movement are not applicable to other shaft designs. As an outlook, varying the shaft geometry and optimising the shape of the bone according to the anatomy would result in a more detailed model.

In this work, the presence of tensile muscular forces was assumed. In some single cases, a clinically observed telescoping effect of fragment dislocation into the humeral shaft is detected. This migration opposite to the muscle contraction leads to the assumption that pressure forces are acting in vivo either from a bulging of SSP or of an intramuscular pressure from the m. deltoideus (DELT). The absence of the DELT has to be discussed for further studies; under physiologic conditions, the muscular contraction while abducting the arm induces a pressure on the subjacent structures [5]. This effect may lead to a pressure on the fragment surfaces and influences dislocation. Whether this effect prevents dislocation or contributes to a stabilised fracture cannot be answered.

A comparison with mentioned experimental study by Dietz et al. [14] (Table 1) is difficult due to different boundary conditions. Alternating forces of 40 N applied to ISP and SSC and constant 40 N for SSP were applied in 25° abduction using one cable circumferentially around the cuff, which is in contrast to our study using 24 N for the SSC, 12 N for the SSP and 6 N for the ISP and two cables around the cuff, one loading cycle and no friction. Nevertheless, a distance of 0.04 mm was seen for the experiment between LT and GT in comparison to results in present investigation of 0.015–0.09 mm. As a consequence, our FE measurements are in the range of that experimental investigation.

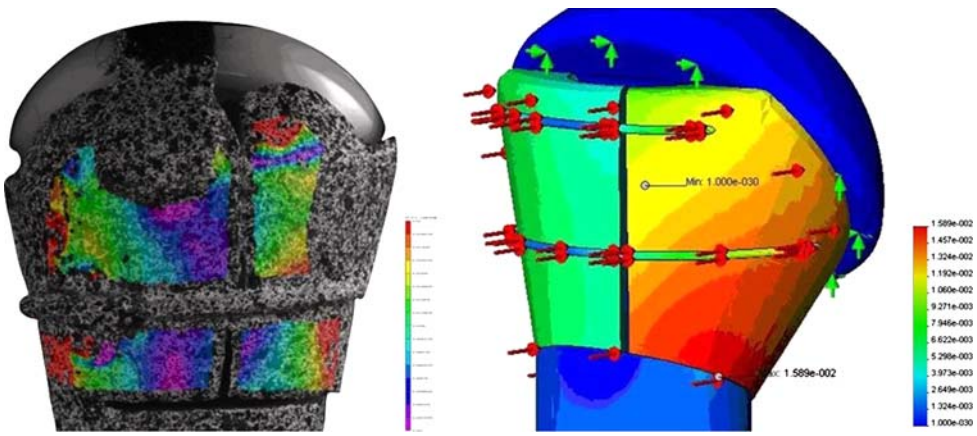

Fig. 5 Strain distribution at the proximal humerus for the experiment (*left*) and simulation (*right*) (a direct comparison is not possible due to a non-uniform scaling)

5 Conclusion

This work showed that we meet requirements to answer the present questions by a FE evaluation of fragment stability in case of hemiarthroplasty. Obviously, an experimental validation of the present study is planned to confirm these findings. Further design modifications of cerclage types and orientations could be pre-evaluated by this mathematical model to reduce extensive and time-consuming experimental testing using cadavers.

Appendix

To validate our FE results, we performed a strain mapping on the bone surface using speckle interferometry (Limess Ltd, Germany). The geometry of the artificial bone model and the fracture lines were chosen according to the solids in the FE analysis (Fig. 5). Polyurethane foam was used as artificial bone material (FR 6715, last-a-foam, General Plastics, Tacoma US, 0.24 g/cm^3, specified in ASTM F1839-97. A commercially available two-camera system was used performing surface speckle interferometry (Vic3D, Limess Ltd.). The speckles were applied on the surface of the artificial bone by a black paint brushing. Local displacements were calculated using Vic-3D-Software based on a vector displacement field of the single speckle dots using an iterative algorithm. For the locations P1–P4 strain values were evaluated. Totally $n = 3$ measurements were done for both the fractured and the healthy humerus.

Based on 100% strain for the healed subject, the fractured bone revealed only 12% strain in the experimental strain mapping for the predetermined location P1. This is somehow in agreement to the results in the FE calculations, except that the strains in the FE analysis for the fractured humerus were four times smaller (Fig. 6).

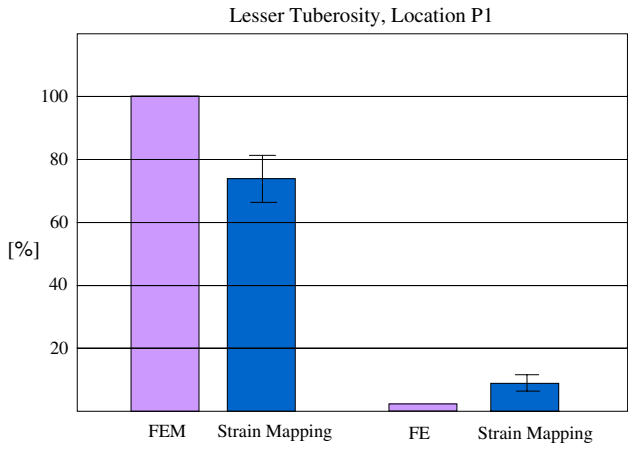

Fig. 6 Experimental and computed strain values at the lesser tuberosity; a decreased strain for the fractured bone is seen in the experiment and simulation

References

1. Abu-Rajab RB et al (2006) Re-attachment of the tuberosities of the humerus following hemiarthroplasty for four-part fracture. J Bone Joint Surg Br 88(11):1539–1544. doi:10.1302/0301-620X.88B11.18246
2. Agorastides I et al (2007) Early versus late mobilization after hemiarthroplasty for proximal humeral fractures. J Shoulder Elbow Surg 16(3 Suppl):S33–S38. doi:10.1016/j.jse.2006.07.004
3. Andreykiv A et al (2005) Bone ingrowth simulation for a concept glenoid component design. J Biomech 38(5):1023–1033. doi:10.1016/j.jbiomech.2004.05.044
4. Bauer TW, Schils J (1999) The pathology of total joint arthroplasty. II. Mechanisms of implant failure. Skeletal Radiol 28(9):483–497. doi:10.1007/s002560050552
5. Billuart F et al (2006) Biomechanics of the deltoideus. Surg Radiol Anat 28(1):76–81. doi:10.1007/s00276-005-0058-8
6. Boileau P et al (2002) Tuberosity malposition and migration: reasons for poor outcomes after hemiarthroplasty for displaced fractures of the proximal humerus. J Shoulder Elbow Surg 11(5):401–412. doi:10.1067/mse.2002.124527
7. Bono CM et al (2001) Effect of displacement of fractures of the greater tuberosity on the mechanics of the shoulder. J Bone Joint Surg Br 83(7):1056–1062. doi:10.1302/0301-620X.83B7.10516
8. Bosch U et al (1998) Outcome after primary and secondary hemiarthroplasty in elderly patients with fractures of the proximal humerus. J Shoulder Elbow Surg 7(5):479–484. doi:10.1016/S1058-2746(98)90198-7
9. Boss AP, Hintermann B (1999) Primary endoprosthesis in comminuted humeral head fractures in patients over 60 years of age. Int Orthop 23(3):172–174. doi:10.1007/s002640050339
10. Brooks CH, Revell WJ, Heatley FW (1993) Vascularity of the humeral head after proximal humeral fractures. An anatomical cadaver study. J Bone Joint Surg Br 75(1):132–136
11. Buchler P et al (2002) A finite element model of the shoulder: application to the comparison of normal and osteoarthritic joints. Clin Biomech (Bristol, Avon) 17(9–10):630–639. doi:10.1016/S0268-0033(02)00106-7
12. De Wilde LF et al (2004) A new prosthetic design for proximal humeral fractures: reconstructing the glenohumeral unit. J Shoulder Elbow Surg 13(4):373–380. doi:10.1016/j.jse.2004.01.018
13. Demirhan M et al (2003) Prognostic factors in prosthetic replacement for acute proximal humerus fractures. J Orthop Trauma 17(3):181–188. doi:10.1097/00005131-200303000-00004 discussion 188–9
14. Dietz SO et al (2008) Tuberosity fixation in shoulder arthroplasty—biomechanical and CT-findings. In: 21st congress of the European Society of the Shoulder and the Elbow, 2008. Congress Abstract, Brugge, Belgium
15. Dines DM, Warren RF (1994) Modular shoulder hemiarthroplasty for acute fractures. Surgical considerations. Clin Orthop Relat Res (307):18–26
16. Frankle MA, Mighell MA (2004) Techniques and principles of tuberosity fixation for proximal humeral fractures treated with hemiarthroplasty. J Shoulder Elbow Surg 13(2):239–247. doi:10.1016/S1058-2746(02)00041-1
17. Gerber C, Schneeberger AG, Vinh TS (1990) The arterial vascularization of the humeral head. An anatomical study. J Bone Joint Surg Am 72(10):1486–1494

18. Goldman RT et al (1995) Functional outcome after humeral head replacement for acute three- and four-part proximal humeral fractures. J Shoulder Elbow Surg 4(2):81–86. doi:10.1016/S1058-2746(05)80059-X
19. Gronhagen CM et al (2007) Medium-term results after primary hemiarthroplasty for comminute proximal humerus fractures: a study of 46 patients followed up for an average of 4.4 years. J Shoulder Elbow Surg 16(6):766–773. doi:10.1016/j.jse.2007.03.017
20. Gupta S, van der Helm FC (2004) Load transfer across the scapula during humeral abduction. J Biomech 37(7):1001–1009. doi:10.1016/j.jbiomech.2003.11.025
21. Hartsock LA et al (1998) Shoulder hemiarthroplasty for proximal humeral fractures. Orthop Clin North Am 29(3):467–475. doi:10.1016/S0030-5898(05)70022-5
22. Hasan SS et al (2002) Characteristics of unsatisfactory shoulder arthroplasties. J Shoulder Elbow Surg 11(5):431–441. doi:10.1067/mse.2002.125806
23. Hawkins RJ, Switlyk P (1993) Acute prosthetic replacement for severe fractures of the proximal humerus. Clin Orthop Relat Res (289):156–160
24. Hessmann MH, Rommens PM (2001) Osteosynthesis techniques in proximal humeral fractures. Chirurg 72(11):1235–1245. doi:10.1007/s001040170026
25. Hoffmeyer P (2002) The operative management of displaced fractures of the proximal humerus. J Bone Joint Surg Br 84(4):469–480. doi:10.1302/0301-620X.84B4.13394
26. Kollig E et al (2003) Primary hemiarthroplasty after complex fracture of the humeral head—functional late results. Zentralbl Chir 128(2):125–130. doi:10.1055/s-2003-37766
27. Kralinger F et al (2004) Outcome after primary hemiarthroplasty for fracture of the head of the humerus. A retrospective multicentre study of 167 patients. J Bone Joint Surg Br 86(2):217–219. doi:10.1302/0301-620X.86B2.14553
28. Kraulis J, Hunter G (1976) The results of prosthetic replacement in fracture-dislocations of the upper end of the humerus. Injury 8(2):129–131. doi:10.1016/0020-1383(76)90048-6
29. Loew M et al (2006) Influence of the design of the prosthesis on the outcome after hemiarthroplasty of the shoulder in displaced fractures of the head of the humerus. J Bone Joint Surg Br 88(3):345–350. doi:10.1302/0301-620X.88B3.16909
30. Maldonado ZM et al (2003) Straining of the intact and fractured proximal humerus under physiological-like loading. J Biomech 36(12):1865–1873. doi:10.1016/S0021-9290(03)00212-4
31. Mansat P et al (2004) Shoulder arthroplasty for late sequelae of proximal humeral fractures. J Shoulder Elbow Surg 13(3):305–312. doi:10.1016/j.jse.2004.01.020
32. Meyer C et al (2005) The arteries of the humeral head and their relevance in fracture treatment. Surg Radiol Anat 27(3):232–237. doi:10.1007/s00276-005-0318-7
33. Mighell MA et al (2003) Outcomes of hemiarthroplasty for fractures of the proximal humerus. J Shoulder Elbow Surg 12(6):569–577. doi:10.1016/S1058-2746(03)00213-1
34. Naranja RJ Jr, Iannotti JP (2000) Displaced three- and four-part proximal humerus fractures: evaluation and management. J Am Acad Orthop Surg 8(6):373–382
35. Orr TE, Carter DR (1985) Stress analyses of joint arthroplasty in the proximal humerus. J Orthop Res 3(3):360–371. doi:10.1002/jor.1100030313
36. Pilliar RM, Lee JM, Maniatopoulos C (1986) Observations on the effect of movement on bone ingrowth into porous-surfaced implants. Clin Orthop Relat Res (208):108–113
37. Reuther F, Muller S, Wahl D (2007) Management of humeral head fractures with a trauma shoulder prosthesis: correlation between joint function and healing of the tuberosities. Acta Orthop Belg 73(2):179–187
38. Robinson CM et al (2003) Primary hemiarthroplasty for treatment of proximal humeral fractures. J Bone Joint Surg Am 85-A(7):1215–1223
39. Schmachtenberg E (2001) Comparative biomechanical examination on the conventional AO-T plate and the humerus fixator plate with the finite element method. Materialwiss Werkstofftech 32:121–125. doi:10.1002/1521-4052(200102)32:2<121::AID-MAWE121>3.0.CO;2-Z
40. Stableforth PG (1984) Four-part fractures of the neck of the humerus. J Bone Joint Surg Br 66(1):104–108
41. Tanner MW, Cofield RH (1983) Prosthetic arthroplasty for fractures and fracture-dislocations of the proximal humerus. Clin Orthop Relat Res (179):116–128
42. van der Helm FC (1994) Analysis of the kinematic and dynamic behavior of the shoulder mechanism. J Biomech 27(5):527–550. doi:10.1016/0021-9290(94)90064-7
43. Wolf JH (1995) Julis Wolff and his "law of bone remodeling". Orthopade 24(5):378–386
44. Zyto K, Kronberg M, Brostrom LA (1995) Shoulder function after displaced fractures of the proximal humerus. J Shoulder Elbow Surg 4(5):331–336. doi:10.1016/S1058-2746(95)80016-6